Spectrally Multiplexed Upconversion Detection With C-Band Pump and Signal Wavelengths

Michael Silver, Paritosh Manurkar, Yu-Ping Huang, Carsten Langrock, Martin M. Fejer, *Member*, *IEEE*, Prem Kumar, *Fellow*, *IEEE*, and Gregory S. Kanter, *Member*, *IEEE*

***Abstract*— We demonstrate a multiplexing scheme for upconversion-based single-photon detection using a waveguide with multiple phase-matching peaks. Two different signal wavelengths are upconverted using two distinct pump wavelengths, where all the wavelengths are in the 1550-nm band. Background photon generation rates $< 10^{-4}$ per pulse with high internal conversion efficiencies are observed using 20-ps-long pump pulses.**

***Index Terms*— Nonlinear optical devices, photodetectors, optical detectors, optical waveguides, multiplexing.**

I. Introduction

NONLINEAR frequency conversion can be used to translate the frequency of a photon while preserving its quantum state [1]. This process can be used to enable high quality, low cost, silicon-based single-photon detectors to function in the telecommunications bands [2]. The promise of higher detection efficiency and better temporal resolution than offered by telecommunications-band single photon avalanche detectors (SPADs) was long hampered by increased background noise generated in the frequency conversion process [3]. It has recently been demonstrated that by moving to appropriately long pump wavelengths, a low background count level can be maintained since unwanted photons from pump down-conversion are eliminated and background photons generated via Raman scattering are greatly reduced [4]. However, when detecting photons in the lowest loss fiber transmission band near 1550 nm the corresponding pump wavelength for low noise upconversion is $>$1800 nm [4]. This is an inconvenient wavelength band that is far less developed than the 1550 nm band, thus impacting the cost and practicality of upconversion detection of telecom band photons.

An emerging application of nonlinear frequency conversion employs pump pulses shaped by an optical arbitrary waveform generator (OAWG) [5] to tailor the temporal mode of the frequency converted signal [6]. This allows temporal mode-resolved single-photon counting (MRPC) as well as the measurement of superpositions of modes [6], [7] which is an essential characteristic in various quantum-optical measurements. A straight-forward implementation of MRPC uses a cascade of upconversion devices pumped by independently shaped pump pulses [8], but the accumulation of coupling loss greatly diminishes the utility of this design. A potential solution is to embed multiple phase-matching peaks in a single waveguide [9]–[12]. This would allow multiple overlapping signal temporal modes of a fixed mean wavelength to be converted to different wavelengths using multiple pump pulses having different wavelengths and spectro-temporal profiles [9]. OAWGs are well developed near 1550 nm. For instance, high speed dynamic pulse shaping has been demonstrated, and commercial OAWGs are available [5], [13]. In principle, such technology could be adapted to the longer wavelengths required for low noise upconversion of 1550-nm band signals, but to our knowledge commercial devices at such wavelengths are currently not available.

We report on an upconversion-based single-photon detector (SPD) with pump and signal pulses in the convenient 1550-nm band. The close pump-to-signal wavelength separation allows operation inside the first major Raman scattering band of Lithium Niobate [14] thereby providing a different mechanism to control Raman scattering than operating at widely spaced wavelengths that fall outside the Raman scattering bands. We show that when the pump-to-signal wavelength separation is kept fairly close ($<$30 nm), it is possible to keep background noise at a level on par with traditional telecom-band-sensitive SPADs. The system allows shorter temporal gate windows than electrically-gated SPADs as the gate duration is specified by the optical pump pulse width (20 ps). An upconversion waveguide with multiple apodized phase-matching peaks is used to convert two different signal wavelengths to two distinct sum-frequency wavelengths. Apodization refers to a technique used to suppress sidelobes in the phase-matching curves, though it also decreases the overall conversion, by tapering the effective nonlinear coupling at the ends of the waveguide [15]. Using multiple pumps and signals in a single waveguide may be useful for multiplexing pulsed signals of different pulse rates and is a first step towards leveraging multiple phase-matching peaks for more complex measurements such as temporal MRPC.

II. Experimental Setup

The second-harmonic generation (SHG) small signal transfer functions of the periodically-poled lithium niobate (PPLN)

Manuscript received February 17, 2017; revised April 13, 2017; accepted May 1, 2017. Date of publication May 10, 2017; date of current version June 13, 2017. This work was supported by the DARPA Quiness Program under Grant W31P4Q-13-1-0004. *(Corresponding author: Michael Silver.)*

M. Silver, P. Kumar, and G. S. Kanter are with the Center for Photonic Communication and Computing, Department of Electrical Engineering and Computer Science, Northwestern University, Evanston, IL 60208 USA (e-mail: michaelsilver2015@u.northwestern.edu; kumarp@northwestern.edu; gregory.kanter@northwestern.edu).

P. Manurkar was with Northwestern University, Evanston, IL 60208 USA. He is now with NIST Boulder, Boulder, CO 80305 USA (e-mail: paritoshmanurkar2013@u.northwestern.edu).

Y.-P. Huang is with the Stevens Institute of Technology, Hoboken, NJ 07030 USA (e-mail: yhuang5@stevens.edu).

C. Langrock and M. M. Fejer are with Stanford University, Stanford, CA 94305 USA (e-mail: langrock@stanford.edu; fejer@stanford.edu).

Color versions of one or more of the figures in this letter are available online at http://ieeexplore.ieee.org.

Digital Object Identifier 10.1109/LPT.2017.2703083

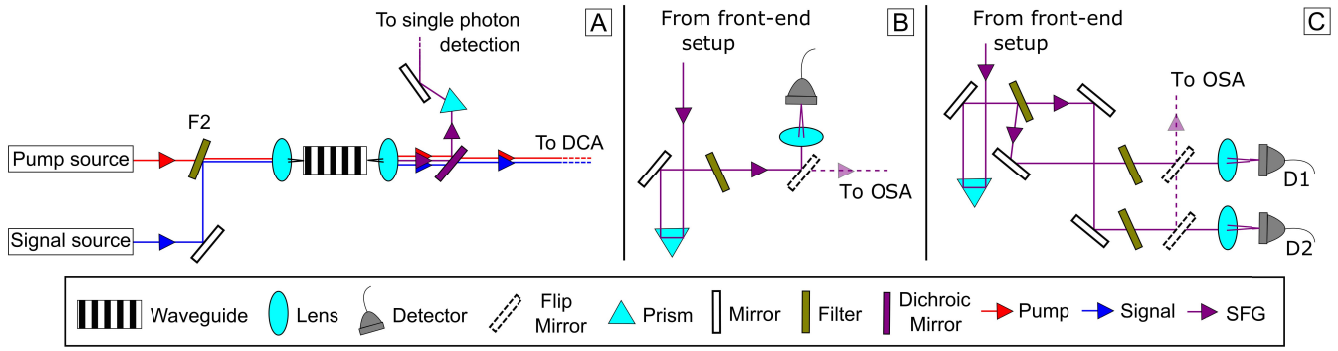

Fig. 1. (Color online) The experimental setup. (A) The front-end coupling to waveguide and separation of C-band from the sum-frequency generation (SFG). Filter F2 combines the pump and signal. (B) The single-peak experiment SFG detection, (C) and multi-peak experiment SFG detection. DCA, digital communications analyzer; OSA, optical spectrum analyzer.

waveguides used in the experiments are shown in Fig. 2. The apodized single-peak waveguide exhibits a peak conversion efficiency of $\simeq$1000 %/W and has suppressed sidelobes. The pump for the single-peak experiments was set at 1550.1 nm while the signal wavelength was changed to observe different system conversion efficiencies and noise characteristics. The multi-peak waveguide has five apodized, 5-nm separated phase-matching peaks. Two pumps, $\lambda_{P1} = 1549.23$ nm and $\lambda_{P2} = 1554.34$ nm, and corresponding signals, $\lambda_{S1} = 1533.54$ nm and $\lambda_{S2} = 1537.51$ nm, were between adjacent phase-matching peaks to generate two sum-frequency generated (SFG) signals at $\lambda_{SFG1} = 770.67$ nm and $\lambda_{SFG2} = 772.94$ nm, respectively. The waveguide peaks chosen have conversion efficiencies of $\eta_1 = 245$ %/W and $\eta_2 = 261$ %/W. Some degradation of performance of these waveguides was due to the anti-reflection coating process and possible photorefractive changes due to milliwatt-level SHG. It was found that 127 mW peak pump power was required for 91% SFG conversion for the single-peak waveguide and 566 mW peak pump power was required for 89% SFG conversion in the multi-peak waveguide.

The experiment employed a common front-end for both the single-peak and multi-peak experiments, with an appropriately modified back-end filtering configuration, as shown in Fig. 1. An OAWG (Finisar: WaveShaper 1000S) was used to shape the signal and pump pulses from 20 GHz input optical frequency combs. The pump and signal were then optically amplified and separated into two distinct fiber ports using a fiber add-drop filter. The signal was passed through a tunable attenuator to control the power injected into the waveguide. The pump was further amplified and additional filtering was applied to remove unwanted amplified spontaneous emission and Raman scattering on both the signal and the pump before both ports were collimated and combined at a free space filter (F2). The pump and signal were then coupled into the waveguide. After the waveguide, the SFG beam was separated from the C-band pump and signal beams using a dichroic mirror and a prism and was further filtered before detection. The C-band pump and signal were coupled to fiber, separated, and signal depletion was measured on a digital sampling oscilloscope (DSO: Agilent-83485B) with a 30-GHz bandwidth.

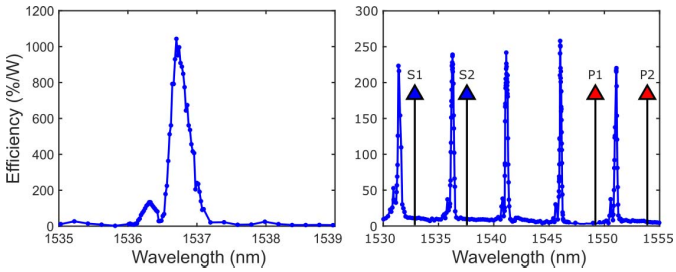

Fig. 2. Single-peak (left) and multi-peak (right) waveguide SHG transfer functions. The position of the signals and pumps is indicated by the labeled triangles.

The SFG filtering and detection setup differed slightly for the single-peak and multi-peak experiments, as is shown in Fig. 1B and C, respectively. For the single-peak setup, the SFG was spatially and spectrally filtered using a bandpass filter (BPF: Semrock LL01-780-25). The filter has >90% transmission at an angle-tunable wavelength near 780 nm, a passband of 3 nm, and an optical density >5. The SFG was then focused onto a single-photon counting module (Excelitas SPCM-AQRH-14). Signal depletion and noise was recorded as a function of pump power at both classical as well as single-photon signal levels.

In the multi-peak experiment, the two SFG signals were separated by the same BPF's used in the single-peak experiment by passing one SFG wavelength and reflecting the other. The two SFG signals then propagated in two spatially independent channels, were further filtered, and focused onto separate SPCMs. Detector 1 (D1) was used to measure the SFG from pump 1 - signal 1 (P1S1) while the SFG from pump 2 - signal 2 (P2S2) was focused onto detector 2 (D2). These two paths will now be referred to as channel 1 and channel 2 respectively. The conversion efficiency, pump-generated noise, and cross-talk between the two channels were then measured.

III. Results

A. Single-Peak Experiment

The pump-generated noise and SFG conversion efficiencies were recorded at various pump powers and pump-signal wavelength separations ($\Delta\lambda$). Pump and signal pulses were

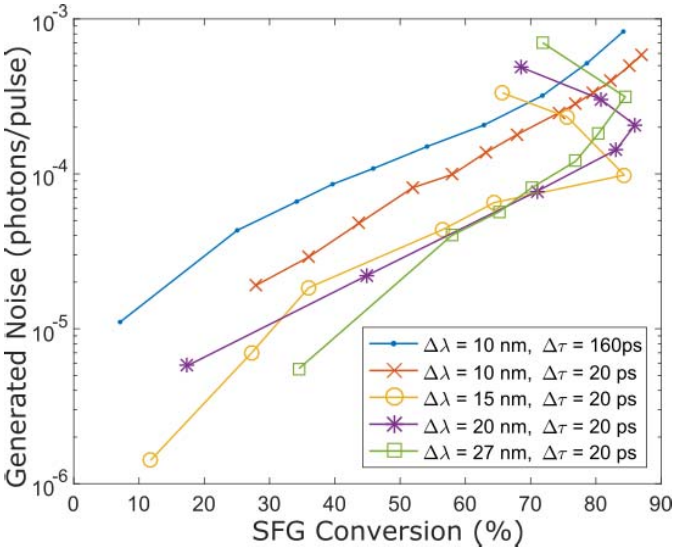

Fig. 3. Generated noise photons/pulse vs. SFG conversion in the single-peak waveguide for two pump widths $\Delta\tau$ and various pump-to-signal wavelength separations $\Delta\lambda$. Back conversion is observed for the 15, 20, and 27 nm cases when overdriving the conversion process.

generated either by directly carving 160 ps full width at half maximum ($\Delta\tau$) pulses at 50 MHz using an external modulator or by using the OAWG to shape $\Delta\tau = 15$ ps signal pulses and $\Delta\tau = 20$ ps pump pulses. A pulse-picker following the OAWG reduced the pulse repetition rate from 20 GHz to 1.25 GHz. The generated noise is stated in photons/pulse exiting the waveguide vs. conversion efficiency, where conversion efficiency is calculated based on the measured signal depletion. The conversion efficiency derived from signal depletion was determined to be within 1 dB of the SFG conversion efficiency under all experimental conditions. The overall system efficiency was also calculated using the waveguide coupling and propagation losses (53%), filtering loss (58%), detector efficiency (65%), and the pump power-dependent SFG conversion efficiency.

To align the SPCM module, a known low power input signal was injected into the waveguide and the expected count rate on the SPCM was calculated. The measured and expected count rate differed by < 1 dB for every value of $\Delta\tau$ and $\Delta\lambda$ for which data was taken. This result also further verifies that signal depletion is a good proxy for conversion efficiency.

One source of background noise is Raman scattering in the waveguide that is subsequently upconverted. Given the ~0.3-nm-wide phase-matching bandwidth and using $2B\Delta\tau \simeq 1$ to determine the temporal width of a single mode in the waveguide, where B is the 3-dB optical bandwidth set by the waveguide SFG phase-matching bandwidth, it is expected that 160-ps-long pump pulses will upconvert many Raman modes and thus generate more noise. This was confirmed by the experiments, which were therefore primarily conducted with pump pulses of $\Delta\tau = 20$ ps. At $\Delta\lambda < 10$ nm, increased generated noise photons/pulse were measured which could be due to the nearby SHG leaking through the back-end filters.

In all cases, peak SFG conversion efficiencies greater than 80% were observed. Low noise in the SFG band was achieved over 10 nm$< \Delta\lambda <$27 nm, and short $\Delta\tau$'s that occupy nearly a single temporal mode. Figure 3 shows the five cases that yielded the highest conversion efficiencies and the least generated noise photons. At $\Delta\lambda = 15$ nm, an SFG efficiency (system efficiency) of 84% (16%) with 10^{-4} noise-generated photons/pulse was observed. Operating the system at a lower pump power reduces the conversion efficiency but it also reduces the noise-generated photons, for example, at a conversion efficiency of 65% (13%) only 6.5×10^{-5} noise photons/pulse were observed. The noise equivalent power (NEP) for the detection system was calculated using the definition for APDs provided by Eraerds et al. [16]. Using a pump with $\Delta\tau = 20$ ps and SFG conversion efficiency greater than 80% (15%) the lowest NEP was found to be 5.6×10^{-16} (W/$\sqrt{Hz}$) at $\Delta\lambda = 15$ nm.

B. Multi-Peak Experiment

The pump and signal-pair wavelengths were chosen to be ≈15-nm apart since low noise at that value of $\Delta\lambda$ was observed in the single-peak experiment. The pump wavelengths were between two adjacent phase-matching peaks (see Fig. 2) to avoid high pump SHG. Signals were placed symmmetrically on the opposite side (15 nm away) of two phase-matching peaks to generate high SFG. It was observed that in these regions the generated noise photons could vary over 10 dB when the pump wavelength changed by ±0.2 nm. This could be due to SHG from parasitic side peaks. The pump wavelengths and waveguide temperature were fine tuned to minimize the pump-induced noise in the SFG band while maintaning high conversion efficiencies.

For a fixed waveguide length, the peak conversion efficiency is inversely proportional to the number of phase-matching peaks. The multi-peaked waveguide therefore requires higher pump powers for a given conversion efficiency, and thus also generates more noise.

The generated noise photons approaches 10^{-4} photons/pulse with an internal conversion efficiency ≈54% (11%) for both P1S1 and P2S2 systems as shown in Fig. 4. Peak conversion efficiencies >80% (15%) were achieved with ≈10^{-3} noise photons/pulse for both channels. The crosstalk between the channels was characterized by measuring the upconversion of the pump-signal combination matched to a given channel vs the upconversion under the same pump with a signal wavelength at the adjacent channel. The efficiency of detecting signal 2 in channel 1 was 61 times less than the efficiency of signal 1 in channel 1. Similarly the detection efficiency of signal 1 upconversion in channel 2 was 124 times less than the efficiency of measuring signal 2 in channel 2.

The right plot in Fig. 4 shows the noise generated in channel 1 vs conversion efficiency when both P1 and P2 pulses are on and temporally overlapped with each other. The total noise level is 3-5 dB higher than the sum of the noise photons/pulse when only one pump is turned on at a time. This suggests a pump interaction is generating background noise. When the pump pulses are sufficiently temporally separated, the noise level returns to a simple sum rule, Fig. 5. The exact

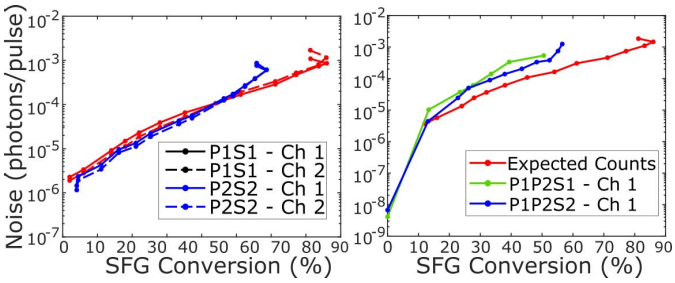

Fig. 4. (Color online) Generated noise vs conversion efficiency of the multi-peak waveguide system for both pumps and their phase-matched signal wavelengths in channels 1 and 2, respectively (left). The expected and measured noise for D1 with both pumps on and either signal injected into the waveguide (right).

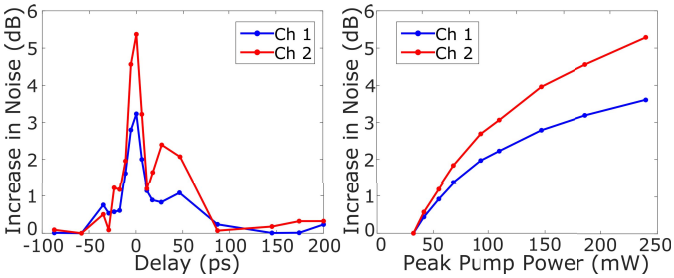

Fig. 5. (Color online) Increased noise due to pump interactions for both channels as a function of time delay between the pumps. (Left) Increased noise as a function of time delay between the pumps. The secondary peak 50 ps away from the main peak is due to imperfect pump pulse picking. (Right) Increased noise as a function of peak pump power with overlapping pump pulses.

mechanism of this added noise still needs to be determined, but is possibly a cascaded interaction such as the SHG of P1 interacting with P2 to create new frequency components in the C-band which are subsequently upconverted. We expect the effect would be mitigated by employing a double-peaked phase matching profile, and could be eliminated by temporally interleaving the S1/S2 signals. Additionally, if the S1/S2 pulse rates are independent, then the overall temporal overlap of the pumps would be reduced by a factor related to the duty cycle, leading to a similar reduction in the extra noise factor.

IV. Conclusion

We demonstrate that in the pulsed mode of operation, upconversion-based single-photon detection using C-band pump and signal pulses can be competitive with C-band-sensitive SPADs, typically generating background photons at a rate $\sim 10^{-4}$ per pulse with $>50\%$ internal conversion efficiency. The pump and signal wavelength separation can be varied by >10 nm with minimal change in the generated noise. The optical gating using 20-ps pulses in this system gives more flexibility than electrical pulse gating, and uses convenient telecom-band pump components. Moreover, we exploit an upconversion waveguide with multiple phase-matching peaks to demonstrate the simultaneous upconversion of two multiplexed signal wavelengths using two different pump wavelengths. Multiple phase-matching peaks may be useful for multiplexing or more complex applications such as temporal mode-resolved photon detection. Using two separate pump wavelengths allows the input signals to be temporally offset, for instance accommodating independent signal pulse rates. Due to a lower effective nonlinearity, the noise levels of multi-peaked devices are somewhat increased, but still have $\sim 10^{-4}$ generated noise photons/pulse a $>30\%$ internal conversion efficiency. Given that upconversion allows telecom-band photons to be detected using Si SPADs, which are generally lower cost and more densely scalable than telecom-band sensitive SPADs, the ability to use a single waveguide to detect multiple low-photon signals may be of technological importance.

Acknowledgment

The authors would like to thank Dr. Nitin Jain for his assistance and support on this work.

References

[1] P. Kumar, "Quantum frequency conversion," *Opt. Lett.*, vol. 15, pp. 1476–1478, Dec. 1990.
[2] A. P. Vandevender and P. G. Kwiat, "High efficiency single photon detection via frequency up-conversion," *J. Modern Opt.*, vol. 51, pp. 1433–1445, Jul. 2009.
[3] C. Langrock, E. Diamanti, R. V. Roussev, Y. Yamamoto, M. M. Fejer, and H. Takesue, "Highly efficient single-photon detection at communication wavelengths by use of upconversion in reverse-proton-exchanged periodically poled $LiNbO_3$ waveguides," *Opt. Lett.*, vol. 30, no. 13, pp. 1725–1727, 2005.
[4] J. S. Pelc *et al.*, "Long-wavelength-pumped upconversion single-photon detector at 1550 nm: Performance and noise analysis," *Opt. Exp.*, vol. 19, pp. 21445–21456, Aug. 2011.
[5] S. T. Cundiff and A. M. Weiner, "Optical arbitrary waveform generation," *Nature Photon.*, vol. 4, pp. 760–766, Oct. 2010.
[6] A. S. Kowligy *et al.*, "Quantum optical arbitrary waveform manipulation and measurement in real time," *Opt. Exp.*, vol. 22, pp. 27942–27957, May 2014.
[7] P. Manurkar *et al.*, "Multidimensional mode-separable frequency conversion for high-speed quantum communication," *Optica*, vol. 3, no. 12, pp. 1300–1307, 2016.
[8] Y.-P. Huang and P. Kumar, "Mode-resolved photon counting via cascaded quantum frequency conversion," *Opt. Lett.*, vol. 38, pp. 468–470, Feb. 2013.
[9] V. G. Velev, C. Langrock, P. Kumar, M. M. Fejer, and Y. P. Huang, "Selective manipulation of overlapping quantum modes," in *Proc. IEEE Photon. Soc. Summer Topical Meeting Ser.*, Montreal, QC, Canada, Jul. 2014, pp. 138–139.
[10] M. H. Chou, K. R. Parameswaran, and M. M. Fejer, "Multiple-channel wavelength conversion by use of engineered quasi-phase-matching structures in $LiNbO_3$ waveguides," *Opt. Lett.*, vol. 24, no. 16, pp. 1157–1159, 1999.
[11] M. Asobe, O. Tadanaga, H. Miyazawa, Y. Nishida, and H. Suzuki, "Multiple quasi-phase-matched $LiNbO_3$ wavelength converter with a continuously phase-modulated domain structure," *Opt. Lett.*, vol. 28, no. 7, pp. 558–560, 2003.
[12] J. S. Pelc, P. S. Kuo, O. Slatery, L. Ma, X. Tang, and M. M. Fejer, "Dual-channel, single-photon upconversion detector at 1.3 μm," *Opt. Exp.*, vol. 20, no. 17, pp. 19075–19087, 2012.
[13] A. M. Weiner, "Ultrafast optical pulse shaping: A tutorial review," *Opt. Commun.*, vol. 284, pp. 3669–3692, Jul. 2011.
[14] A. Ridah, P. Bourson, M. D. Fontana, and G. Malovichko, "The composition dependence of the Raman spectrum and new assignment of the photons in $LiNbO_3$," *J. Phys. B, Condens. Matter*, vol. 9, pp. 9683–9687, May 1997.
[15] J. Huang, X. P. Xie, C. Langrock, R. V. Roussev, D. S. Hum, and M. M. Fejer, "Amplitude modulation and apodization of quasiphase-matched interactions," *Opt. Lett.*, vol. 31, pp. 604–606, Mar. 2006.
[16] P. Eraerds, M. Legré, J. Zhang, H. Zbinden, and N. Gisin, "Photon counting OTDR: Advantages and limitations," *J. Lightw. Technol.*, vol. 28, no. 6, pp. 952–964, Mar. 15, 2010.